Plasma kallikrein modulates immune cell trafficking during neuroinflammation via PAR2 and bradykinin release

Kerstin Göbel[a,1,2], Chloi-Magdalini Asaridou[a,2], Monika Merker[a], Susann Eichler[a], Alexander M. Herrmann[a], Eva Geuß[b], Tobias Ruck[a], Lisa Schüngel[a,c], Linda Groeneweg[a], Venu Narayanan[a], Tilman Schneider-Hohendorf[a], Catharina C. Gross[a], Heinz Wiendl[a], Beate E. Kehrel[c], Christoph Kleinschnitz[d,3], and Sven G. Meuth[a,3]

[a]Clinic of Neurology, Institute of Translational Neurology, University of Münster, 48149 Münster, Germany; [b]Department of Neurology, University Hospital Würzburg, 97080 Würzburg, Germany; [c]Clinic of Anesthesiology, Intensive Care and Pain Medicine, Experimental and Clinical Haemostasis, University of Münster, 48149 Münster, Germany; and [d]Department of Neurology, University Hospital Essen, 45147 Essen, Germany

Edited by Lawrence Steinman, Stanford University School of Medicine, Stanford, CA, and approved November 19, 2018 (received for review June 11, 2018)

Blood–brain barrier (BBB) disruption and transendothelial trafficking of immune cells into the central nervous system (CNS) are pathophysiological hallmarks of neuroinflammatory disorders like multiple sclerosis (MS). Recent evidence suggests that the kallikrein-kinin and coagulation system might participate in this process. Here, we identify plasma kallikrein (KK) as a specific direct modulator of BBB integrity. Levels of plasma prekallikrein (PK), the precursor of KK, were markedly enhanced in active CNS lesions of MS patients. Deficiency or pharmacologic blockade of PK renders mice less susceptible to experimental autoimmune encephalomyelitis (a model of MS) and is accompanied by a remarkable reduction of BBB disruption and CNS inflammation. In vitro analysis revealed that KK modulates endothelial cell function in a protease-activated receptor-2–dependent manner, leading to an up-regulation of the cellular adhesion molecules Intercellular Adhesion Molecule 1 and Vascular Cell Adhesion Molecule 1, thereby amplifying leukocyte trafficking. Our study demonstrates that PK is an important direct regulator of BBB integrity as a result of its protease function. Therefore, KK inhibition can decrease BBB damage and cell invasion during neuroinflammation and may offer a strategy for the treatment of MS.

plasma kallikrein | coagulation | multiple sclerosis | neuroinflammation | EAE

Autoimmune disorders of the central nervous system (CNS), such as multiple sclerosis (MS), are mediated by different immune components (1, 2). It is assumed that autoreactive T cells formed in the periphery migrate across the disrupted blood–brain barrier (BBB) and induce inflammatory lesions within the brain parenchyma, leading to demyelination and axonal damage. This cell trafficking is a tightly regulated process that not only depends on the activation status of leukocytes, but also is governed by the BBB via the expression of cellular adhesion molecules, tight junction proteins, and different chemokines (3–5). The key components of the BBB are highly specialized brain endothelial cells that express low levels of adhesion molecules and form close intracellular tight junctions to limit trans- and paracellular trafficking of cells and molecules (4). However, structural integrity of the BBB can become compromised under inflammatory conditions through the up-regulation of adhesion molecules and the rearrangement of tight junction proteins, such that transendothelial trafficking increases (5, 6).

Recent evidence suggests that other factors not traditionally considered to be components of the immune system might also be involved in the MS pathophysiology. Some constituents of the coagulation and the kallikrein-kinin system (KKS) are thought to contribute to MS and its animal model, experimental autoimmune encephalomyelitis (EAE) (7–12). Plasma prekallikrein (PK) is the precursor of plasma kallikrein (KK) and, together with factor XII (FXII) and high-molecular-weight kininogen (HK), is an important part of the KKS (13). Activation of PK by activated FXII (FXIIa) leads to cleavage of HK, releasing the proinflammatory peptide bradykinin (BK). At the same time, KK can activate FXII in a positive feedback loop, thereby leading to both activation of the intrinsic coagulation cascade and the proinflammatory KKS (14, 15). Additionally, KK may interact with cell-surface–associated receptors, such as the protease-activated receptors 1 (PAR1) and 2 (PAR2) (16).

As KK has this dual mode of action (inflammation and coagulation), and has recently been identified as an important regulator during ischemic neurodegeneration (17), we investigated its role in neuroinflammation and the potential underlying mechanisms of action. Moreover, we analyzed the therapeutic potential of KK inhibition in EAE models and were able to demonstrate that KK regulates immune cell trafficking to the CNS by modulating BBB function.

Results

PK Deficiency Provides Protection from CNS Autoimmunity. To determine if KK is relevant during neuroinflammation in vivo, we first analyzed the plasma, lymph nodes (LNs), spleen, cerebrospinal fluid (CSF), and CNS of naive and myelin oligodendrocyte

Significance

Transendothelial trafficking of immune cells into the central nervous system (CNS) is a pathophysiological hallmark of neuroinflammatory disorders like multiple sclerosis (MS). Recent evidence suggests that the coagulation and kallikrein-kinin cascade might participate in this process. Here, we identify plasma kallikrein (KK) as a direct modulator of blood–brain barrier function in a protease-activated receptor-2–dependent manner, amplifying leukocyte trafficking into the CNS. Consequently, a deficiency of plasma prekallikrein (PK), the precursor of KK, renders mice less susceptible to experimental autoimmune encephalomyelitis (model of MS). Furthermore, PK levels were markedly enhanced in CNS lesions of MS patients. In summary, our study indicates that KK inhibition can decrease cell invasion during neuroinflammation and may offer a strategy to combat MS.

Author contributions: K.G. designed research; K.G., C.-M.A., M.M., S.E., A.M.H., E.G., T.R., L.S., L.G., V.N., T.S.-H., and C.C.G. performed research; K.G., H.W., B.E.K., C.K., and S.G.M. analyzed data; and K.G. and S.G.M. wrote the paper.

The authors declare no conflict of interest.

This article is a PNAS Direct Submission.

[1]To whom correspondence should be addressed. Email: kerstin.goebel@ukmuenster.de.

[2]K.G. and C.-M.A. contributed equally to this work.

[3]C.K. and S.G.M. contributed equally to this work.

This article contains supporting information online at www.pnas.org/lookup/suppl/doi:10.1073/pnas.1810020116/-/DCSupplemental.

Published online December 17, 2018.

glycoprotein 35–55 ($MOG_{35–55}$)–immunized WT mice. While PK levels were almost unchanged in the plasma, LNs, and spleen upon EAE induction, PK was significantly increased in the inflamed CNS of immunized mice (Fig. 1 *A* and *B*). Additionally, we found a significant increase of KK, the enzymatic active form of PK, in the plasma and CSF, indicating a potential contribution to EAE pathology (Fig. 1*C*). To evaluate the functional role of KK, we subjected *Klkb1*$^{-/-}$ mice (lacking PK) and their respective WT controls to EAE by immunization with $MOG_{35–55}$. Clinical scores were evaluated daily over a 35-d period. PK deficiency was associated with a milder disease course, while disease onset was unaltered (Fig. 1*D*). In line with this finding, inflammatory infiltrates and demyelination were reduced in $MOG_{35–55}$–immunized *Klkb1*$^{-/-}$ mice compared with WT controls on the maximum of disease (d_{max}) (Fig. 1*E*). To test if the protective effect can be attributed to PK deficiency, *Klkb1*$^{-/-}$ animals were reconstituted with human PK revealing restored susceptibility to EAE (Fig. 1*F*).

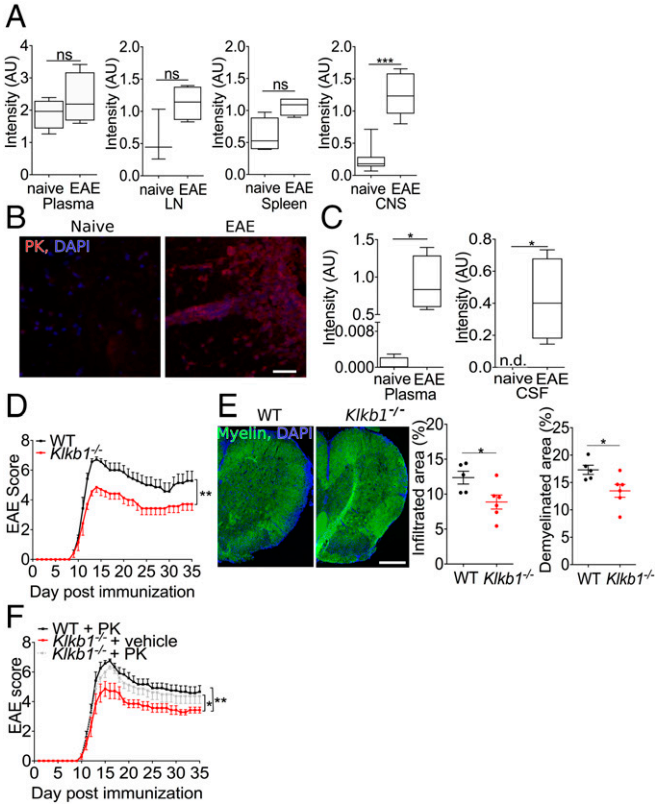

Fig. 1. PK-deficient (*Klkb1*$^{-/-}$) mice are protected from EAE. (*A*) PK levels in the plasma, LNs, spleen, and CNS of naive and $MOG_{35–55}$–immunized WT animals. Immunoblots were independently replicated from five different animals using β-actin as a loading control (nonparametric Mann–Whitney *U* test). (*B*) Histological analysis of spinal cord sections of $MOG_{35–55}$–immunized WT animals at disease maximum. Sections were stained for PK (red) and nucleus (DAPI, blue). (Scale bar, 50 μm.) (*C*) KK levels in the plasma and CSF of naive and $MOG_{35–55}$–immunized WT animals. Immunoblots were independently replicated from four different animals using β-actin as a loading control (nonparametric Mann–Whitney *U* test). (*D*) Active EAE was induced in WT and *Klkb1*$^{-/-}$ mice by immunization with $MOG_{35–55}$. Clinical scores (mean ± SEM) over time are shown (two-way ANOVA). (*E*) Histological analysis of spinal cord sections from WT and *Klkb1*$^{-/-}$ animals at disease maximum. Sections were stained with fluoromyelin (green) and nucleus (DAPI, blue) to evaluate inflammatory foci and demyelination. (Scale bar, 200 μm.) Data are presented as mean ± SEM (n = 3 slices of five to six mice per group, nonparametric Mann–Whitney *U* test). (*F*) Clinical scores (mean ± SEM) over time of WT, *Klkb1*$^{-/-}$, and *Klkb1*$^{-/-}$animals reconstituted with PK (*Klkb1*$^{-/-}$ + PK) (two-way ANOVA). $^{*}P < 0.05$, $^{**}P < 0.01$, $^{***}P < 0.001$. ns, not significant.

PK Deficiency Leads to Decreased Immune Cell Trafficking in the Course of Neuroinflammation. We evaluated the immune cell distribution in different compartments of *Klkb1*$^{-/-}$ and WT animals. The distribution of different immune cell subsets from *Klkb1*$^{-/-}$ and WT mice was similar under $MOG_{35–55}$–immunized conditions (day 10 after immunization) in the blood, spleen, and LNs (*SI Appendix*, Fig. S1 *A–C*). Furthermore, PK deficiency had no influence on proliferation or cytokine production (*SI Appendix*, Fig. S1*D*). However, the number of immune cells infiltrating the CNS was significantly reduced in *Klkb1*$^{-/-}$ compared with WT mice at d_{max} as determined using flow cytometry analyses (Fig. 2*A* and *SI Appendix*, Fig. S2), while the BBB permeability to vascular tracer molecules did not differ between *Klkb1*$^{-/-}$ and WT animals (Fig. 2*B*). In line with this finding, histological studies revealed reduced numbers of $CD3^{+}$ T cells as well as $CD11b^{+}$ macrophages/microglia in *Klkb1*$^{-/-}$ mice compared with WT controls, while the distribution of immune cells when analyzing different CNS regions was undistinguishable (Fig. 2*C* and *SI Appendix*, Fig. S3).

These results were corroborated under in vitro conditions. To exclude any effect in addition to PK deficiency in *Klkb1*$^{-/-}$ mice, we analyzed transendothelial resistance (TER) and capacitance of the cell layer (CcL) in murine brain microvascular endothelial cells (MBMECs) of these mice in comparison with WT controls in parallel. While TER significantly decreased under inflammatory conditions, no additional effect could be achieved by PK deficiency (*SI Appendix*, Fig. S4*A*). In a next step, we examined a potentially direct influence of PK on MBMECs of WT animals. Interestingly, MBMECs were able to activate PK to KK under steady-state and inflammatory conditions in vitro (Fig. 3*A*), leading to a cleavage of the chromogenic KK substrate S2302. However, known activating proteins like prolylcarboxypeptidase and heat shock protein 90 were not detectable in endothelial cells and/or endothelial supernatants (18).

Furthermore, although TER (Fig. 3*B*) and chemokine secretion of MBMECs were unaltered in the presence of PK (*SI Appendix*, Fig. S4*B*) under steady-state and inflammatory conditions, trafficking of leukocytes was significantly enhanced in the presence of PK (Fig. 3*C*), indicating a detrimental direct contribution of PK or its enzymatic active form KK on endothelial cells. This finding was accompanied by a significant upregulation of the adhesion molecules Intercellular Adhesion Molecule 1 (*Icam-1*) and Vascular Cell Adhesion Molecule 1 (*Vcam-1*) in the presence of PK (Fig. 3*D*), while tight junction molecules were unchanged (*SI Appendix*, Fig. S4*C*). These results were confirmed in vivo by immunohistochemistry showing enhanced expression of the ICAM-I and VCAM-I in WT compared with *Klkb1*$^{-/-}$ mice (Fig. 3*E*).

PK Enhances EAE only in Part by Release of BK. KK can cleave FXII to its active form, thereby initiating both the proinflammatory KKS, resulting in BK release, and the intrinsic coagulation cascade, leading to an activation of factor X (FX) and prothrombin, and thereby finally causing fibrin formation (13). There is evidence that the inhibition of active FX (FXa) and thrombin is protective in EAE (11, 19). To exclude that improved EAE outcome is due to different amounts of thrombin and FXa in the plasma and CNS in *Klkb1*$^{-/-}$ mice compared with WT controls, we determined the concentration of both. Plasma and CNS concentrations of FXa and thrombin in *Klkb1*$^{-/-}$ animals were indistinguishable from those of WT animals (*SI Appendix*, Fig. S5*A*). Of note, the amount of thrombin was significantly increased in the inflamed CNS at the peak of disease (*SI Appendix*, Fig. S5*A*), which is in line with earlier publications (20).

We have recently shown that FXII leads to enhanced inflammation during neuroinflammation (12). We therefore analyzed the amount of FXII deposits in the CNS of *Klkb1*$^{-/-}$ and WT animals at d_{max}. Interestingly, the amount of the zymogen did not differ between the groups (*SI Appendix*, Fig. S5*B*). As KK mediates the release of BK from HK, we evaluated the BK

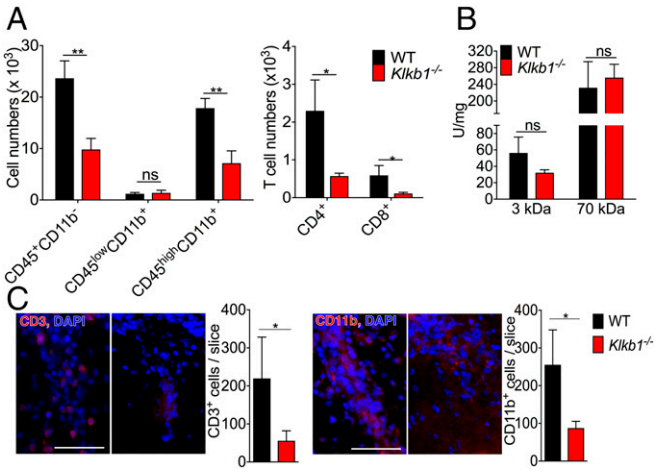

Fig. 2. PK deficiency leads to reduced migration to the CNS. (*A*) Number of brain-infiltrating leukocytes from $MOG_{35–55}$–immunized WT or *Klkb1*$^{-/-}$ mice was evaluated by flow cytometry at d_{max}. (*B*) Quantification of fluorescein–dextran (3 kDa; *Left*) and Texas red–dextran (70 kDa; *Right*) into the CNS 1 h after i.v. application in immunized mice at d_{max}. (*C*) Histological analysis of infiltrated $CD3^+$ T cells and macrophages and microglia ($CD11b^+$) at d_{max}. Representative images of spinal cord sections and corresponding quantifications are shown for WT and *Klkb1*$^{-/-}$ mice. (Scale bars, 100 μm.) In *A*–*C*, data are given as means ± SEM of two independent experiments, each performed in triplicate (six mice per group). Nonparametric Mann–Whitney *U* test or Kruskal–Wallis test with Dunn post hoc analysis in case of multiple comparisons were used. **P* < 0.05, ***P* < 0.01. ns, not significant.

plasma level of naive and $MOG_{35–55}$–immunized animals. As expected, plasma BK levels were almost absent when PK was missing (Fig. 4*A*). In line with this finding, BK levels in the CSF (Fig. 4*A*) and the amount of BK deposits in CNS lesions (Fig. 4*B*) were significantly decreased in *Klkb1*$^{-/-}$ compared with WT animals at d_{max}. As BK can be further cleaved to des-Arg^9-bradykinin, acting primarily via BK receptor 1 (B1R), the receptor known to be relevant in EAE (7, 8), additional studies were performed. Intriguingly, the amount of des-Arg^9-BK deposits was undistinguishable between the groups (Fig. 4*B*).

However, as BK and des-Arg^9-BK are rapidly metabolized and have a very short half-life, we also determined the amount of cleaved HK (cHK) in plasma and CSF. The amount of cHK was significantly reduced in *Klkb1*$^{-/-}$ mice compared with WT controls (Fig. 4*C*), indicating a potential role of BK release in this context. When testing if B1R activation is relevant in vivo, we found that B1R activation with the agonist R838 led only to a partial reconstitution of the EAE phenotype (Fig. 4*D*). Overall, these findings indicate that activation of the KKS inducing the cleavage of HK and the release of BK is not sufficient to completely explain the detrimental effects of PK in autoimmune neuroinflammation.

Other pathways known to be triggered by KK are the cleavage of C3 and C5. Modulation of C3a or C5a has been shown to be relevant in EAE (21). However, C5a serum levels did not differ between WT and *Klkb1*$^{-/-}$ animals, thereby excluding a major pathophysiologic role of this system (*SI Appendix*, Fig. S5*C*).

KK Modulates BBB Function via PAR2. KK can directly act on cells by binding to PAR1, PAR2, and B2R (16, 22). As MBMECs were able to activate PK to KK in vitro (Fig. 3*A*), we evaluated *F2r* (PAR1), *F2rl1* (PAR2), and *B2r* expression in MBMECs from WT animals by Real-Time Reverse Transcription–Polymerase Chain Reaction (rRT-PCR) to identify these receptors as potential targets of KK. Interestingly, while *B2r* expression was unaltered under inflammatory conditions, and *F2r* expression was down-regulated, *F2rl1* expression was up-regulated (*SI Appendix*, Fig. S5*D*). The expression profile was also seen on the protein level on MBMECs (*SI Appendix*, Fig. S5*E*). To address if PK can directly modulate immune cell trafficking, we used different in vitro approaches. Again, enhanced immune cell trafficking was observed when incubating MBMECs of *B2r*$^{-/-}$ or *F2r*$^{-/-}$ animals with PK compared with control (*SI Appendix*, Fig. S5 *F* and *G*). In contrast, no significant difference in migration could be found when using MBMECs of *F2rl1*$^{-/-}$ animals in the presence of PK or vehicle, indicating that PAR2 on endothelial cells is the main receptor mediating the detrimental effects of KK (Fig. 4*E*). To prove that PAR2 is also relevant in vivo, we treated *Klkb1*$^{-/-}$ with a known PAR2-activating peptide. Interestingly, this treatment led to restored susceptibility to EAE, arguing for a direct effect of KK on endothelial cells via PAR2 (Fig. 4*F*).

Pharmacologic Inhibition of KK Protects from EAE in a Clinically Relevant Setting. Since PK deficiency prevented EAE, we investigated whether the effect of PK deficiency could be mimicked by using a blocking antibody (17). Indeed, treatment with the KK antibody when applied after neurological symptom onset significantly attenuated the signs of EAE in WT mice (Fig. 5*A*) and ameliorated

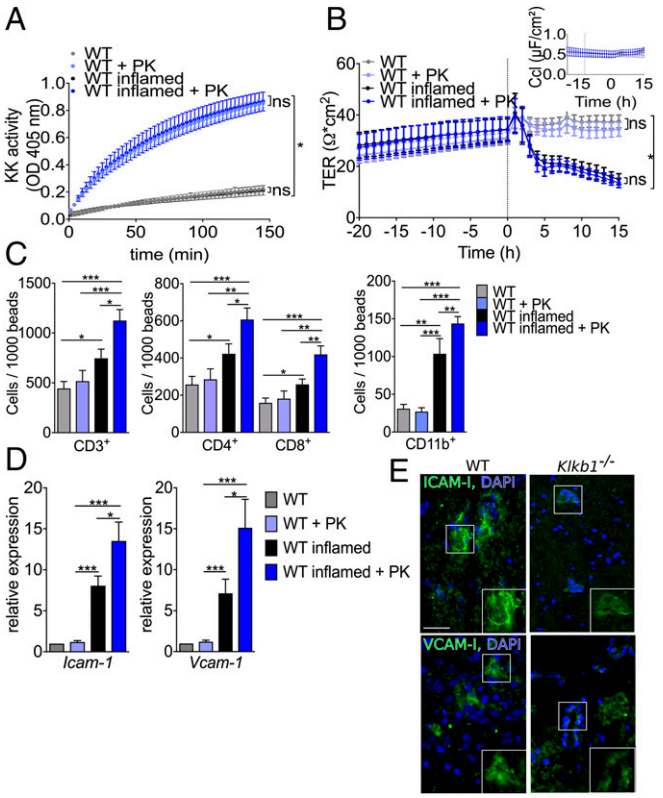

Fig. 3. The presence of PK leads to enhanced migration by up-regulation of adhesion molecules in MBMEC. (*A*) KK activity of WT s in the presence or absence of PK. KK activity was quantified as change in absorption at 405 nm measured at 2-min intervals. Data are shown from one of three experiments, which produced comparable results. (*B*) TER of WT MBMECs in the presence or absence of PK over time. (*Inset*) CcL that was measured in parallel. (*C*) Migration of immune cells across an MBMEC monolayer in the presence or absence of PK under naive and inflammatory conditions. (*D*) rRT-PCR analyses for the adhesion molecules *Icam-1* and *Vcam-1* expression in MBMECs in the presence or absence of PK under naive or inflammatory conditions. (*E*) Histological analysis of ICAM-I and VCAM-I in spinal cord sections for WT and *Klkb1*$^{-/-}$ mice. (Scale bars, 20 μm.) In *B*–*E*, data are given as mean ± SEM of two or three independent experiments, each performed in triplicate. Nonparametric Mann–Whitney *U* test or Kruskal–Wallis test with Dunn post hoc analysis in case of multiple comparisons were used. **P* < 0.05; ***P* < 0.01; ****P* < 0.001; ns, not significant.

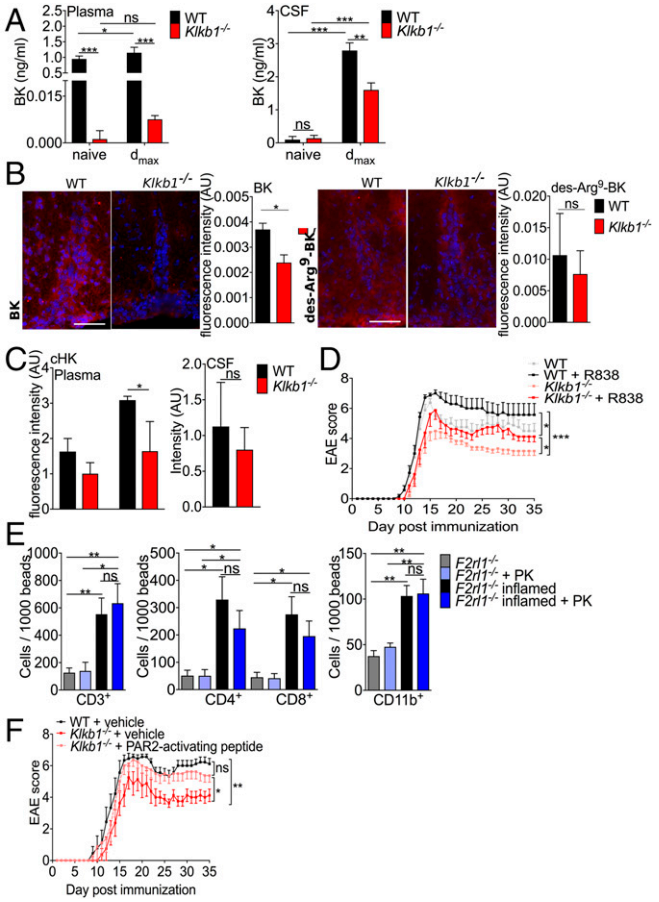

Fig. 4. Plasma KK controls migration via PAR2. (*A*) BK release in plasma and CSF of naive and $MOG_{35–55}$–immunized WT and *Klkb1*$^{-/-}$ animals at d_{max} of EAE. Data are mean ± SEM of 4 vs. 4 animals from one of three independent experiments, each performed in duplicate. (*B*) Immunohistochemical analysis of spinal cord white matter infiltrates for BK and des-Arg9-BK (red, respectively) from EAE mice at d_{max}. Representative images and corresponding quantifications are shown for WT and *Klkb1*$^{-/-}$ mice. Slices were additionally stained to label nuclei (DAPI, blue). (Scale bars, 50 μm.) Data are presented as mean ± SEM ($n = 3$ slices of four to six mice per group, nonparametric Mann–Whitney *U* test). (*C*) cHK level in plasma of naive and $MOG_{35–55}$–immunized WT and *Klkb1*$^{-/-}$ animals. Immunoblots were independently replicated from four different animals using β-actin as a loading control. (*D*) Active EAE was induced in WT and *Klkb1*$^{-/-}$ mice by immunization with $MOG_{35–55}$ and were treated with the BK 1 receptor activator R838. Clinical scores (mean ± SEM) over time of two independent EAE experiments are shown (two-way ANOVA). (*E*) Migration of immune cells across a MBMEC monolayer of *F2rl1*$^{-/-}$ animals in the presence or absence of PK under naive and inflammatory conditions. (*F*) Clinical EAE scores (mean ± SEM) of WT and *Klkb1*$^{-/-}$ mice treated with vehicle or a PAR2-activating peptide are shown (two-way ANOVA). In *A* and *D*, data are given as mean ± SEM. Kruskal–Wallis test with Dunn post hoc analysis was used. *$P < 0.05$; **$P < 0.01$; ***$P < 0.001$; ns, not significant.

cellular inflammation and demyelination (day 35 after immunization; Fig. 5*B*), while the distribution of different immune cell subsets in spleen and LNs was similar under $MOG_{35–55}$–immunized conditions (day 35 after immunization; Fig. 5*C*). These findings suggest that KK inhibition is also effective in clinically relevant settings.

PK Is Up-Regulated in Active CNS Lesions of MS Patients. To assess whether PK is also relevant in humans, we analyzed plasma from individuals with different forms of MS [clinically isolated syndrome (CIS), relapsing-remitting MS (RRMS), primary progressive MS (PPMS), and secondary progressive MS (SPMS)] (*SI Appendix*, Table S1). PK plasma levels were unchanged in patients suffering from all different forms of MS compared with healthy donors (HDs) (Fig. 6*A*). However, enhanced PK depositions were observed in the CNS of individuals with MS, but not in controls (Fig. 6*B* and *SI Appendix*, Fig. S6*A*). As murine data suggest a regulatory function of PK on endothelial cells, we performed transmigration assays using human brain microvascular endothelial cells (HBMECs). Again, endothelial cells were able to activate PK to KK (Fig. 6*C*). In line with the murine data, PK incubation did not alter endothelial cell production of chemokines (*SI Appendix*, Fig. S6*B*). However, the expression of *Icam-I* was significantly enhanced, while tight junction proteins were unchanged (Fig. 6*D*). Interestingly, PK led to an extensive enhancement of leukocyte trafficking across HBMEC layers (Fig. 6*E*), indicating a significant role of KK, not only in mice, but also in humans.

Discussion

Brain capillary endothelial cells are the major structural constituents of the BBB and are critically involved in regulating directional cell flux into the CNS and vice versa. Here we show that PK is a critical regulator of inflammatory cell invasion during autoimmune CNS diseases. Genetic depletion or pharmacological inhibition of PK or KK, respectively, protects mice from EAE by preserving the structural integrity of the BBB and by reducing transendothelial leukocyte trafficking. Reduced expression of cellular adhesion molecules was identified as an underlying mechanism. Importantly, these findings could be reproduced by pharmacological inhibition of KK in WT mice even after EAE onset. Furthermore, we detected a strong expression of PK in EAE lesions at d_{max}, as well as in active human MS lesions, but not in healthy CNS tissue.

Cellular adhesion molecules like ICAM-I and VCAM-I play a decisive role in the dynamic regulation of transendothelial cell migration (23, 24) and are up-regulated at the BBB during EAE and MS (4). Accordingly, a specific blockade of these molecules, e.g., by monoclonal antibodies, is a promising strategy to treat inflammatory CNS diseases (24–26). We could demonstrate that PK deficiency or KK inhibition down-regulates the gene expressions of

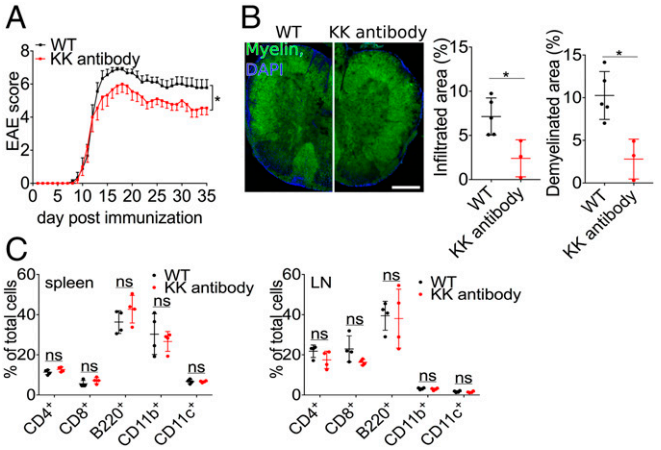

Fig. 5. Plasma KK blockade protects from neuroinflammation. (*A*) Clinical scores (mean ± SEM) of myelin oligodendrocyte glycoprotein 35–55–immunized WT mice treated with KK-inhibiting antibody or vehicle starting at the first day of neurologic symptoms (two-way ANOVA). (*B*) Histological analysis of spinal cord sections from WT animals treated with PK-inhibiting antibody or vehicle. Sections were stained with fluoromyelin (green) and DAPI (blue) to evaluate inflammatory foci and demyelination. (Scale bar, 200 μm.) ($n = 3$ slices of three to six mice per group, nonparametric Mann–Whitney *U* test.) (*C*) Cells were isolated from spleen and LNs of WT treated with vehicle or KK-inhibiting antibody day 35 postinduction of EAE, stained with the indicated markers and analyzed by flow cytometry. In *B* and *C*, data are given as mean ± SEM of two independent experiment. *$P < 0.05$; ns, not significant.

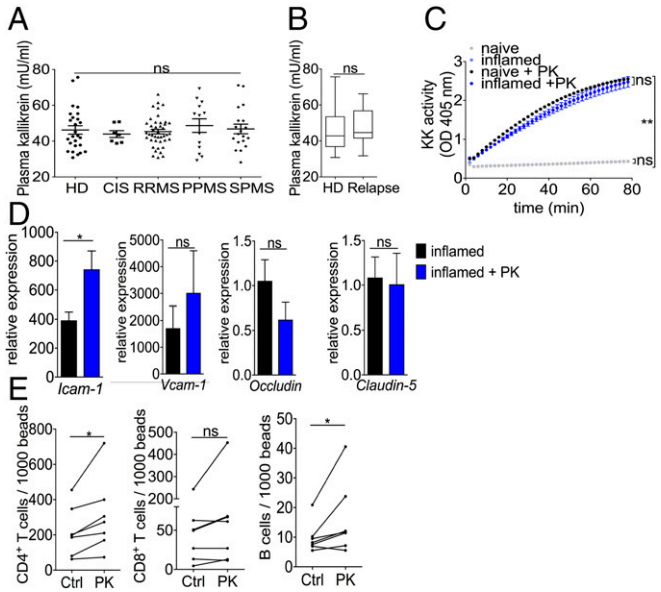

Fig. 6. Evidence for the involvement of plasma KK in human autoimmune CNS inflammation. (*A*) PK serum levels in individuals with CIS and MS compared with HDs. (*B*) Histological analysis of CNS tissue from individuals with MS or from control. Data are given as mean ± SEM. Nonparametric Mann–Whitney *U* test was used. (*C*) KK activity of HBMECs in the presence or absence of PK. KK activity was quantified as change in absorption at 405 nm measured at 2-min intervals. Data are shown from one of three experiments, which produced comparable results (two-way ANOVA). (*D*) rRT-PCR analyses for the adhesion molecules *Icam-1*, *Vcam-1*, *occluding*, and *claudin-5* expression in HBMECs in the presence or absence of PK under naive or inflammatory conditions. (*E*) Migration of immune cells of seven different donors across a HBMEC monolayer in the presence or absence of PK under naive and inflammatory conditions. (Wilcoxon matched-pairs signed rank test). In *D*, data are given as mean ± SEM of two independent experiments, each performed in triplicate. Nonparametric Mann–Whitney *U* test were used. $*P < 0.05$, $**P < 0.01$; ns, not significant.

ICAM-I and VCAM-I in human and mouse cerebral endothelial cells. It is well established that targeted interruption of kinin receptor-mediated pathways predominantly exerts antiinflammatory effects. PK is central to triggering the proinflammatory KKS, leading to the formation of BK. BK's physiological and pathophysiological effects are mediated by two distinct BK receptors (27). Human studies revealed that B1R is expressed on circulating lymphocytes and infiltrating T cells during active episodes of MS. Moreover, B1R can be found on endothelial cells within MS plaques (28–30). In the EAE model, contradictory reports exist with regard to the relevance of B1R and B2R (7, 8).

Apart from triggering the KKS, there is increasing evidence that some coagulation factors may be involved in autoimmune disorders such as MS, inflammatory bowel disorder, or dermatitis (31–33). Depositions of fibrinogen and the degradation products thereof were found in the CNS or skin of patients with MS or dermatitis (31–33). In the brain, those depositions fostered microglia activation and subsequent plaque formation (10, 33). Moreover, a close correlation between the cerebral or spinal fibrin load and the number of relapses was reported in EAE mice, and anticoagulant administration or fibrinogen depletion reversed the pathology (11, 34). Furthermore, inhibition of other coagulation factors like thrombin or FXa led to an amelioration of neuroinflammation in animal models (11, 19).

However, while the disruption of the BBB in PK-deficient mice was attenuated, we found that, for this effect, the coagulation system was not required. Moreover, B1R activation was not sufficient to reconstitute the EAE phenotype. These unexpected observations led us to hypothesize that KK might directly affect the BBB via PAR1 or PAR2. Each member of the PAR family of G-protein–coupled receptors contains an internal ligand within the N terminus that is exposed upon proteolysis by enzymatic cleavage by specific serine proteases (16). Depending on their location, these receptors regulate diverse processes like inflammation, cell migration, and hemostasis (16). Indeed, isolated MBMECs expressed both PAR1 and PAR2, with PAR2 being up-regulated under inflammatory conditions. Most notably, KK influenced migration only in the presence of PAR2 on MBMECs. From a translational perspective, KK blockade had a beneficial effect on disease severity and progression. Sharing the advantage with FXII of not leading to bleeding complications, PK blockade could be a promising strategy for MS therapy (17).

Overall, our study identifies KK as a key regulator of brain endothelial cells during neuroinflammation. Targeted inhibition of KK might become a promising approach to influence the BBB and thereby impact the disease progression in MS. Further studies in relevant preclinical disease models are needed.

Methods

Detailed methods are provided in *SI Appendix, Supplementary Methods*.

Mice. BK receptor B2-deficient (*B2r*$^{-/-}$), PAR1-deficient (*F2r*$^{-/-}$), PAR2-deficient (*F2rl1*$^{-/-}$), and PK-deficient (*Klkb1*$^{-/-}$) mice have been described previously (7, 17, 35). All transgenic mice were backcrossed into a C57BL/6 background for at least 10 generations. C57BL/6 mice (Charles River) aged 8–12 wk served as controls (WT). All experiments were approved by the local authorities (LANUV) and were conducted in accordance with the German laws and regulations for animal care.

Induction of EAE. Active EAE was induced and evaluated as previously outlined (12). For reconstitution experiments, a subgroup of WT and *Klkb1*$^{-/-}$ mice were injected daily i.v. with purified human PK (4 mg/kg; Enzyme Research Laboratories) (17). Pharmacological modulation of B1R was performed using the selective B1R agonist R838 (1 mg/kg; Tocris) (8, 36, 37) administered daily intraperitoneally (7). For activation of PAR2, a subgroup of *Klkb1*$^{-/-}$ animals was treated with a PAR2-activating peptide (SLIGRL-NH_2, 1.5 mg/kg; Bachem) or control peptide (LSIGRL-NH_2; Bachem) (38). KK-blocking antibody (Biozol) or control IgG (vehicle; Biozol) was administered by daily i.v. injections starting 1 d after the appearance of the first clinical signs (17).

Histology and Immunohistochemistry. At the d_{max}, spinal cords and brains were removed, embedded, and cut into 10-μm sections. For human CNS tissue, human autopsy and biopsy material from MS and control patients was obtained from The UK Multiple Sclerosis Tissue Bank (Division of Neuroscience and Mental Health). Cryofixed tissues from MS and control patients were cut into 10-μm sections. Immunohistochemistry was performed as previously described (12). All patients gave informed consent in accordance with the Declaration of Helsinki and a protocol approved by the Ethic Committee of the University of Münster.

BBB Permeability in Vivo. For analysis of BBB permeability, 100 μL of 25 mg·ml^{-1} Texas red–dextran or fluorescein–dextran in PBS were injected i.v. into the tail vein of immunized WT and *Klkb1*$^{-/-}$ mice as previously described (39). After 1 h, brain and spinal cord were removed and homogenized in 1% Triton-X100 in PBS and centrifuged for 30 min at 16,000 × *g*. The supernatants were used for quantification with the TECAN Infinite M200PRO at 595/615 nm (for Texas red–dextran) or 494/521 nm (for fluorescein–dextran).

Leukocyte Isolation and Stimulation. LNs and/or spleen cells from *Klkb1*$^{-/-}$, WT mice, and animals treated with the PK antibody or vehicle were isolated from naive or immunized animals 10 or 35 d after the induction of EAE or at the peak of disease (12). In brief, cells were cultured for 2 d and stimulated with CD3/CD28 beads (cell-to-bead ratio of 2:1; Dynal Biotech) or 10 μg/mL $MOG_{35–55}$.

Flow Cytometry. For the detection of cell-surface markers by flow-activated cell-sorting analysis, single-cell suspensions from murine LNs, spleen, and spinal cord cells of WT and *Klkb1*$^{-/-}$ mice under basal conditions, at d_{10} or d_{max} of EAE, as well as fractioned cell populations and human peripheral blood mononuclear cells, were stained for 30 min at 4 °C with appropriate combinations of indicated fluorescence-labeled monoclonal antibodies in

PBS containing 0.1% NaN_3 and 0.1% BSA. Corresponding isotype controls were used for all stainings.

rRT-PCR and Western Blot. RNA isolation and rRT-PCR were performed as previously described using different TaqMan gene expression assays (Applied Biosystems) (12). Data were calculated using Δct, ΔΔct, and relative quantification ($2^{-\Delta\Delta CT}$).

Western blot analyses was performed as previously described (17, 40). Quantification was performed with the ImageJ software (National Institutes of Health).

Determination of BK, Activated Coagulation Factor, and Complement Levels in Mice. Samples of plasma, CSF, and CNS lysate were taken from mice under basal conditions or at d_{max} of EAE. The CSF was collected as previously described (12). BK and activated coagulation factors (FXa, thrombin) were assessed using ELISA kits (Bradykinin ELISA Kit; Phoenix Pharmaceuticals; FXa ELISA Kit; MyBioSource; Thrombin ELISA Kit; Abcam) according to the manufacturer's instructions. Complement (C5a) detection was performed as previously described (12).

Endothelial Cells, TER, Chemokine Measurement, Migration Assay, and Activation of PK. Isolation of MBMECs was conducted as previously described (7). HBMECs were purchased from PELOBiotech and cultured in precoated (speed coating PELOBiotech) T-75 flasks with endothelial cell medium (ScienCell Research Laboratories). HBMECs (1.0×10^5, passage 5–9) were seeded into precoated (speed coating; PELOBiotech) 3.0-μm-pore polyester transwell inserts (Corning). At day 2–3 after seeding, HBMECs were inflamed (each 100 $U \cdot mL^{-1}$ IFNγ and TNFα; Peprotech, overnight) or left under steady-state conditions and simultaneously treated with human PK (900 nM; Haemochrom Diagnostica) or vehicle (sodium acetate). MBMECs or HBMECs were incubated with 450 nM human PK (Enzyme Research Laboratories) in the presence of 0.6 mM of the chromogenic substrate for plasma KK, S2302 (Chromogenix). Upon addition of the reagents, cells were placed in the TECAN Infinite M200PRO, and absorption at 405 nm was measured at 2-min intervals.

Patients. Fresh blood samples were obtained from 79 MS patients referred to the Clinic of Neurology of the Institute of Translational Neurology at the University of Münster. MS diagnosis was made according to the revised criteria of Polman et al. (41). In parallel, 26 sex- and age-matched HDs were included in the study. PK levels of samples were determined by ELISA (MyBioSource) according to the manufacturer's instructions.

Statistical Methods. To analyze the EAE data, we performed an analysis of variance (ANOVA). Unpaired data were evaluated by a nonparametric Mann–Whitney *U* test or Kruskal–Wallis test with Dunn's post hoc analysis in case of multiple comparisons. For human migration experiments, the Wilcoxon matched-pairs signed rank test was used. In vitro and in vivo data are expressed as mean ± SEM from at least three independent experiments, unless otherwise indicated. Statistical analyses were performed using the Prism software version 5.0 (GraphPad).

ACKNOWLEDGMENTS. We thank V. Schütte, C. Butz, and J. Budde for excellent technical assistance. This work was supported by Else-Kröner-Fresenius-Stiftung Grant 2015_A113 (to K.G.); Deutsche Forschungsgemeinschaft Grants GO2505/1-1 (to K.G.), SFB 688, TPA13 (to C.K.), ME 3283/5-1, and ME 3283/6-1 (to S.G.M.); and the Medical Faculty Münster Young Investigator Group (K.G.).

1. Ganguly D, Haak S, Sisirak V, Reizis B (2013) The role of dendritic cells in autoimmunity. *Nat Rev Immunol* 13:566–577.
2. Bhat R, Steinman L (2009) Innate and adaptive autoimmunity directed to the central nervous system. *Neuron* 64:123–132.
3. Hickey WF, Hsu BL, Kimura H (1991) T-lymphocyte entry into the central nervous system. *J Neurosci Res* 28:254–260.
4. Man S, Ubogu EE, Ransohoff RM (2007) Inflammatory cell migration into the central nervous system: A few new twists on an old tale. *Brain Pathol* 17:243–250.
5. Engelhardt B, Ransohoff RM (2012) Capture, crawl, cross: The T cell code to breach the blood-brain barriers. *Trends Immunol* 33:579–589.
6. Abbott NJ, Patabendige AA, Dolman DE, Yusof SR, Begley DJ (2010) Structure and function of the blood-brain barrier. *Neurobiol Dis* 37:13–25.
7. Göbel K, et al. (2011) Blockade of the kinin receptor B1 protects from autoimmune CNS disease by reducing leukocyte trafficking. *J Autoimmun* 36:106–114.
8. Schulze-Topphoff U, et al. (2009) Activation of kinin receptor B1 limits encephalitogenic T lymphocyte recruitment to the central nervous system. *Nat Med* 15:788–793.
9. Gveric D, Herrera B, Petzold A, Lawrence DA, Cuzner ML (2003) Impaired fibrinolysis in multiple sclerosis: A role for tissue plasminogen activator inhibitors. *Brain* 126: 1590–1598.
10. Adams RA, et al. (2007) The fibrin-derived gamma377-395 peptide inhibits microglia activation and suppresses relapsing paralysis in central nervous system autoimmune disease. *J Exp Med* 204:571–582.
11. Han MH, et al. (2008) Proteomic analysis of active multiple sclerosis lesions reveals therapeutic targets. *Nature* 451:1076–1081.
12. Göbel K, et al. (2016) Blood coagulation factor XII drives adaptive immunity during neuroinflammation via CD87-mediated modulation of dendritic cells. *Nat Commun* 7: 11626.
13. Björkqvist J, Jämsä A, Renné T (2013) Plasma kallikrein: The bradykinin-producing enzyme. *Thromb Haemost* 110:399–407.
14. Schmaier AH (2008) The elusive physiologic role of factor XII. *J Clin Invest* 118: 3006–3009.
15. Schmaier AH (2008) Assembly, activation, and physiologic influence of the plasma kallikrein/kinin system. *Int Immunopharmacol* 8:161–165.
16. Abdallah RT, et al. (2010) Plasma kallikrein promotes epidermal growth factor receptor transactivation and signaling in vascular smooth muscle through direct activation of protease-activated receptors. *J Biol Chem* 285:35206–35215, and erratum (2011) 286:23620.
17. Göb E, et al. (2015) Blocking of plasma kallikrein ameliorates stroke by reducing thromboinflammation. *Ann Neurol* 77:784–803.
18. Shariat-Madar Z, Mahdi F, Schmaier AH (2002) Identification and characterization of prolylcarboxypeptidase as an endothelial cell prekallikrein activator. *J Biol Chem* 277: 17962–17969.
19. Merker M, et al. (2017) Rivaroxaban ameliorates disease course in an animal model of multiple sclerosis. *J Neuroimmunol* 313:125–128.
20. Davalos D, et al. (2014) Early detection of thrombin activity in neuroinflammatory disease. *Ann Neurol* 75:303–308.
21. Strainic MG, Shevach EM, An F, Lin F, Medof ME (2013) Absence of signaling into $CD4^+$ cells via C3aR and C5aR enables autoinductive TGF-β1 signaling and induction of $Foxp3^+$ regulatory T cells. *Nat Immunol* 14:162–171.
22. Hecquet C, Tan F, Marcic BM, Erdös EG (2000) Human bradykinin B(2) receptor is activated by kallikrein and other serine proteases. *Mol Pharmacol* 58:828–836.
23. Dietrich JB (2002) The adhesion molecule ICAM-1 and its regulation in relation with the blood-brain barrier. *J Neuroimmunol* 128:58–68.
24. Greenwood J, Etienne-Manneville S, Adamson P, Couraud PO (2002) Lymphocyte migration into the central nervous system: Implication of ICAM-1 signalling at the blood-brain barrier. *Vascul Pharmacol* 38:315–322.
25. Engelhardt B (2006) Molecular mechanisms involved in T cell migration across the blood-brain barrier. *J Neural Transm (Vienna)* 113:477–485.
26. Rice GP, Hartung HP, Calabresi PA (2005) Anti-alpha4 integrin therapy for multiple sclerosis: Mechanisms and rationale. *Neurology* 64:1336–1342.
27. Albert-Weißenberger C, Sirén AL, Kleinschnitz C (2013) Ischemic stroke and traumatic brain injury: The role of the kallikrein-kinin system. *Prog Neurobiol* 101-102:65–82.
28. Prat A, et al. (2000) Kinin B1 receptor expression and function on human brain endothelial cells. *J Neuropathol Exp Neurol* 59:896–906.
29. Prat A, et al. (2005) Kinin B1 receptor expression on multiple sclerosis mononuclear cells: Correlation with magnetic resonance imaging T2-weighted lesion volume and clinical disability. *Arch Neurol* 62:795–800.
30. Prat A, et al. (1999) Bradykinin B1 receptor expression and function on T lymphocytes in active multiple sclerosis. *Neurology* 53:2087–2092.
31. Adams RA, Schachtrup C, Davalos D, Tsigelny I, Akassoglou K (2007) Fibrinogen signal transduction as a mediator and therapeutic target in inflammation: Lessons from multiple sclerosis. *Curr Med Chem* 14:2925–2936.
32. Reitamo S, Reunala T, Konttinen YT, Saksela O, Salo OP (1981) Inflammatory cells, IgA, C3, fibrin and fibronectin in skin lesions in dermatitis herpetiformis. *Br J Dermatol* 105:167–177.
33. Davalos D, et al. (2012) Fibrinogen-induced perivascular microglial clustering is required for the development of axonal damage in neuroinflammation. *Nat Commun* 3:1227.
34. Akassoglou K, et al. (2004) Fibrin depletion decreases inflammation and delays the onset of demyelination in a tumor necrosis factor transgenic mouse model for multiple sclerosis. *Proc Natl Acad Sci USA* 101:6698–6703.
35. Gyetko MR, Sud S, Chensue SW (2004) Urokinase-deficient mice fail to generate a type 2 immune response following schistosomal antigen challenge. *Infect Immun* 72: 461–467.
36. Austinat M, et al. (2009) Blockade of bradykinin receptor B1 but not bradykinin receptor B2 provides protection from cerebral infarction and brain edema. *Stroke* 40: 285–293.
37. Raslan F, et al. (2010) Inhibition of bradykinin receptor B1 protects mice from focal brain injury by reducing blood-brain barrier leakage and inflammation. *J Cereb Blood Flow Metab* 30:1477–1486.
38. Fiorucci S, et al. (2001) Proteinase-activated receptor 2 is an anti-inflammatory signal for colonic lamina propria lymphocytes in a mouse model of colitis. *Proc Natl Acad Sci USA* 98:13936–13941.
39. Bittner S, et al. (2013) Endothelial TWIK-related potassium channel-1 (TREK1) regulates immune-cell trafficking into the CNS. *Nat Med* 19:1161–1165.
40. Fernández-Orth J, et al. (2017) 14-3-3 proteins regulate K_{2P} 5.1 surface expression on T lymphocytes. *Traffic* 18:29–43.
41. Polman CH, et al. (2011) Diagnostic criteria for multiple sclerosis: 2010 revisions to the McDonald criteria. *Ann Neurol* 69:292–302.